PNAS
www.pnas.org

Supplementary Information for

Conformational equilibrium defines the variable induction of the multidrug-binding transcriptional repressor, QacR

Koh Takeuchi[1,2*], Misaki Imai[3], and Ichio Shimada[1,4*]

[1]Biomedicinal Information Research Center & Molecular Profiling Research Center for Drug Discovery, National Institute of Advanced Industrial Science and Technology, Aomi 2-3-26, Koto-ku, Tokyo 135-0064, Japan.
[2]PRESTO, JST, Aomi 2-3-26, Koto-ku, Tokyo 135-0064, Japan.
[3]Research and Development Department, Japan Biological Informatics Consortium, Aomi 2-3-26, Koto-ku, Tokyo 135-0064, Japan.
[4]Graduate School of Pharmaceutical Sciences, The University of Tokyo, 7-3-1 Hongo, Bunkyo-ku, Tokyo 113-0033, Japan.

[*]**Correspondence to:**
Prof. Ichio Shimada, Ph.D,
Email: shimada@iw-nmr.f.u-tokyo.ac.jp

Koh Takeuchi, PhD,
Email: koh-takeuchi@aist.go.jp

This PDF file includes:

Figures S1 to S11
Tables S1
SI References

www.pnas.org/cgi/doi/10.1073/pnas.1906129116

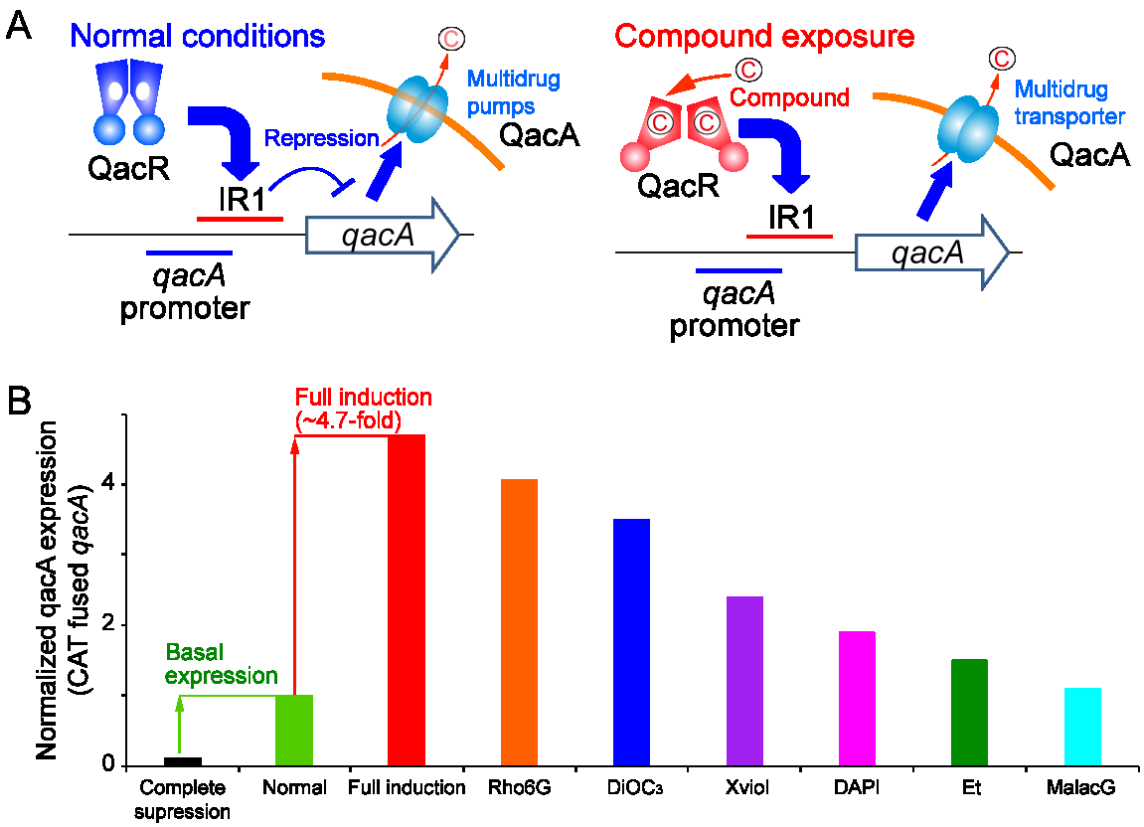

Figure S1. Transcription regulation of the *qacA* gene by QacR. (A) Schematic representation of *qacA* expression by QacR. (Upper) In normal conditions, QacR suppresses the expression of the multidrug transporter QacR by binding to the 28 bp inverted repeat 1 (IR1) operator that overlaps with the *qacA* promoter. (Lower) Upon compound binding, the QacR interaction with IR1 is reduced to induce the expression of QacA. (B) Basal and full induction activities of the *qacA* gene along with those induced by compounds. The expression levels of the CAT fused *qacA* gene in each condition are shown. Complete supression and full induction conditions corresponding to those with the *qacA* promoter and the IR1 operator deletion, respectively. The sequences shared between the *qacA* promoter and the IR1 operator are not modified. The figure is reproduced from the data shown in Grkovic et al.(1, 2)

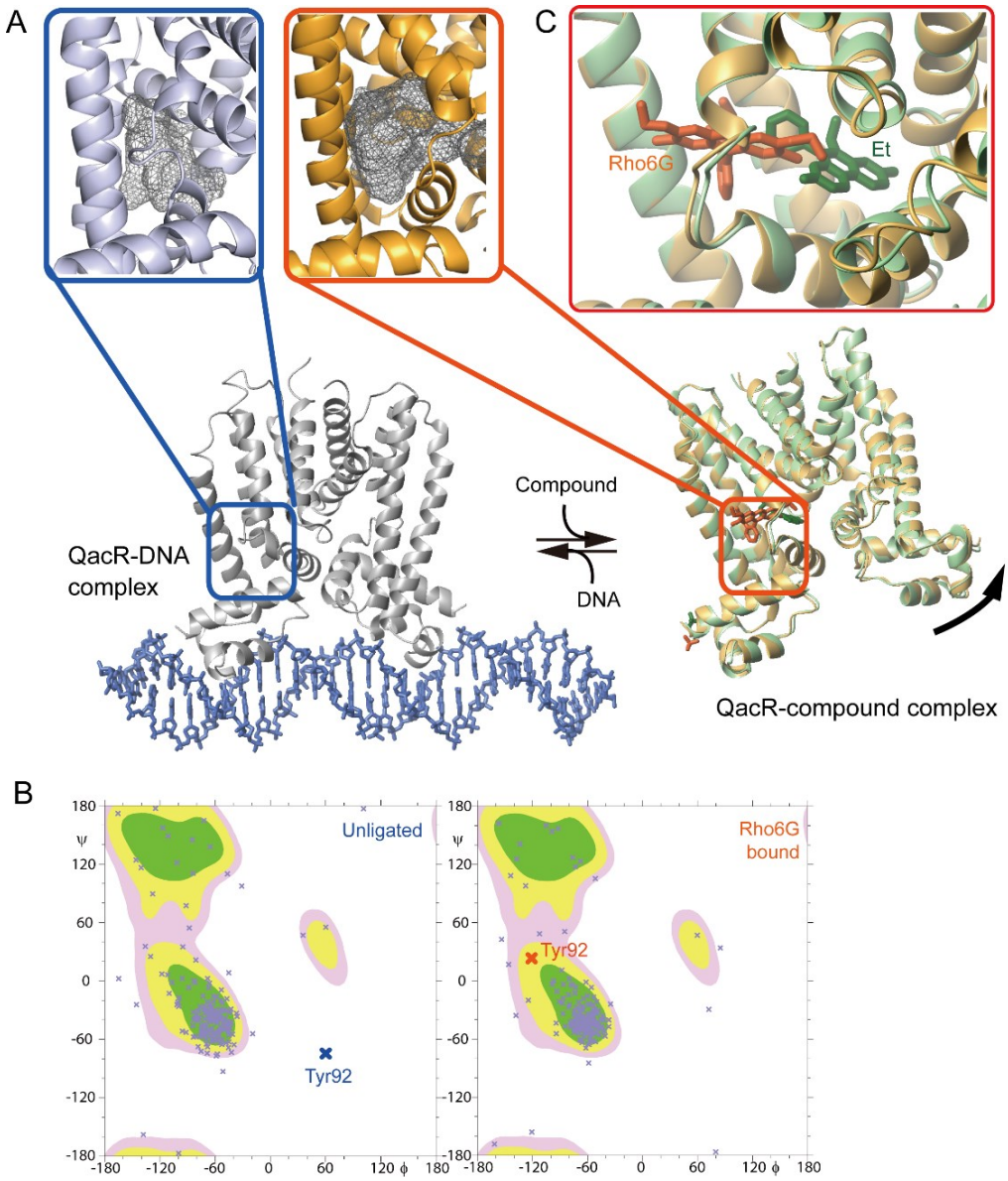

Figure S2. X-ray Structures of QacR in different conditions. (A) QacR strutucre in complex with the IR1 DNA (bottom, left) and compounds (bottom right, Rho6G; orange, Et; green) are shown. The compound-bound structure shows the characteristic expansion of the multidrug binding (MDB) pocket (top, representative structure is for QacR in complex with Rho6G). The shapes of the MDB pockets are indicated by shadow. Rho6G is omitted from the structure for clarity. (B) Dissolution of the Ramachandran outlier at Tyr92 in the Rho6G-bound structure. The energetically unfavorable ϕ angle of Tyr92 mainchain in unligated state is eliminated in in the Rho6G-bound structure. (C) Enlarged view of the MDB pocket of QacR in complex with Rho6G and Et. Although the structures of QacR are almost identical, the compounds are accommodated in distinct but partially overlapping sub-pockets.

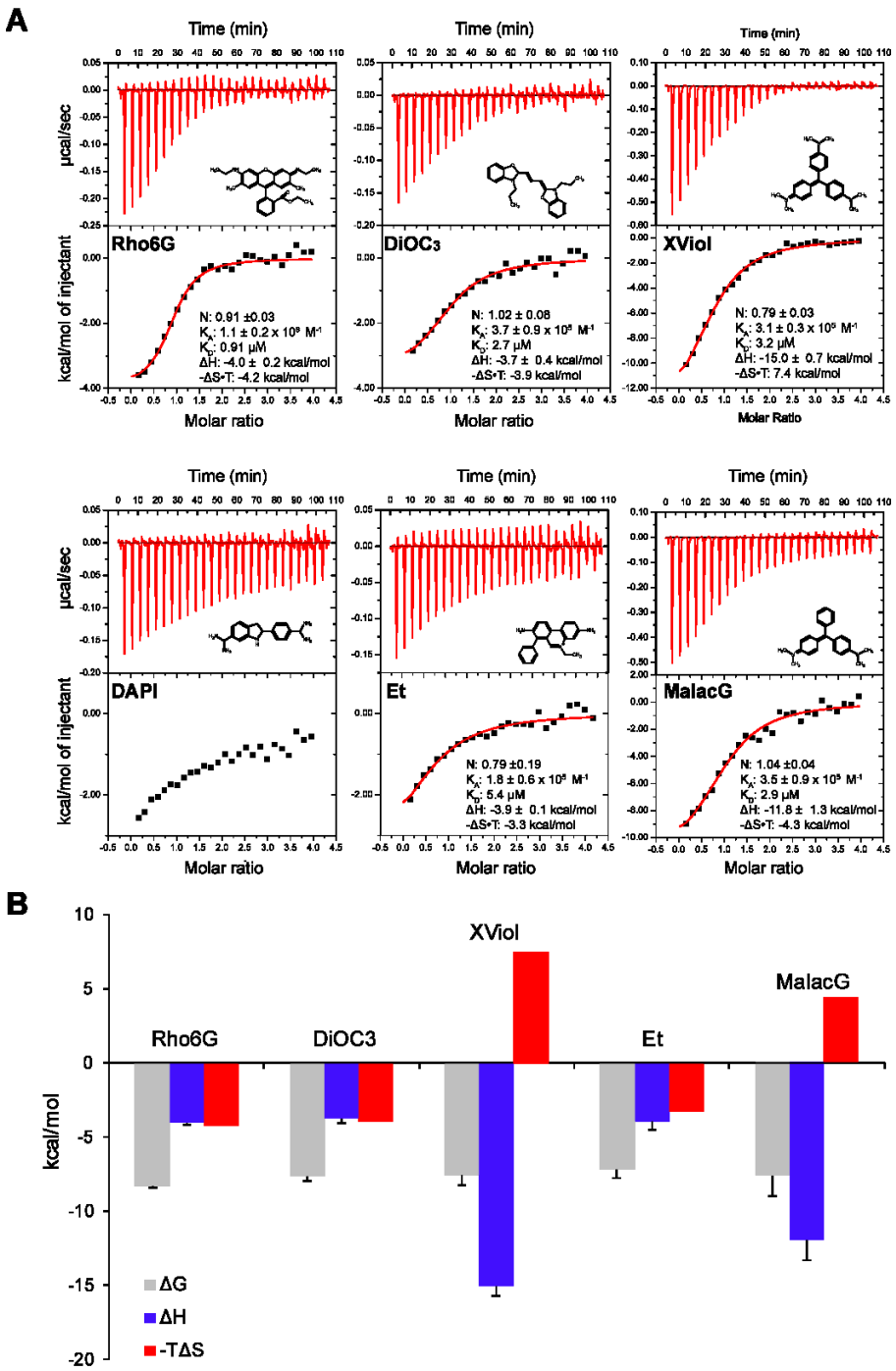

Figure S3. ITC experiment of QacR-compound interactions. (A) Representative ITC profiles for the calorimetric titration of QacR to compound. *N* is the stoichiometry of the QacR subunit to compound (i.e., *N* = 1 means each subunit in the QacR dimer binds to one compound). Calorimetric titrations were performed using a VP-ITC microcalorimeter (MicroCal) at 25 °C. A mutant QacR (C72A/C141S) was used to prevent the cross-linking and oxidation during the experiment that were observed in the WT protein. The double mutant QacR is reportedly fully active and its DNA binding and drug binding properties are essentially identical to those of the WT protein. Protein samples were extensively dialyzed against ITC buffer, containing 10 mM Na-Pi (pH 6.8), 100 mM NaCl, and 5% DMSO. The sample cell was filled with 10 µM Rho6G, and the injection syringe contained 200 µM QacR (subunit concentration). DMSO was added to the

buffer, in order to increase the solubility of the compound. After a preliminary 3 µL injection, 27 subsequent 10 µL injections were performed. The data were subtracted by the titration experiment without compound and fitted using the one-site binding model embedded in Origin 7.0 (MicroCal). (B) Thermodynamic signatures of the compound-QacR interactions are shown. The K_D values and the total enthalpy of the binding deduced from the ITC analyses were used to determine the total free energy change (ΔG) and total enthalpy change (ΔH), respectively. The total entropy change (ΔS) was calculated from the difference between ΔG and ΔH. As there is substantial heat generation even at the end of the titration, the thermodynamic parameters and K_D value for DAPI was not determined.

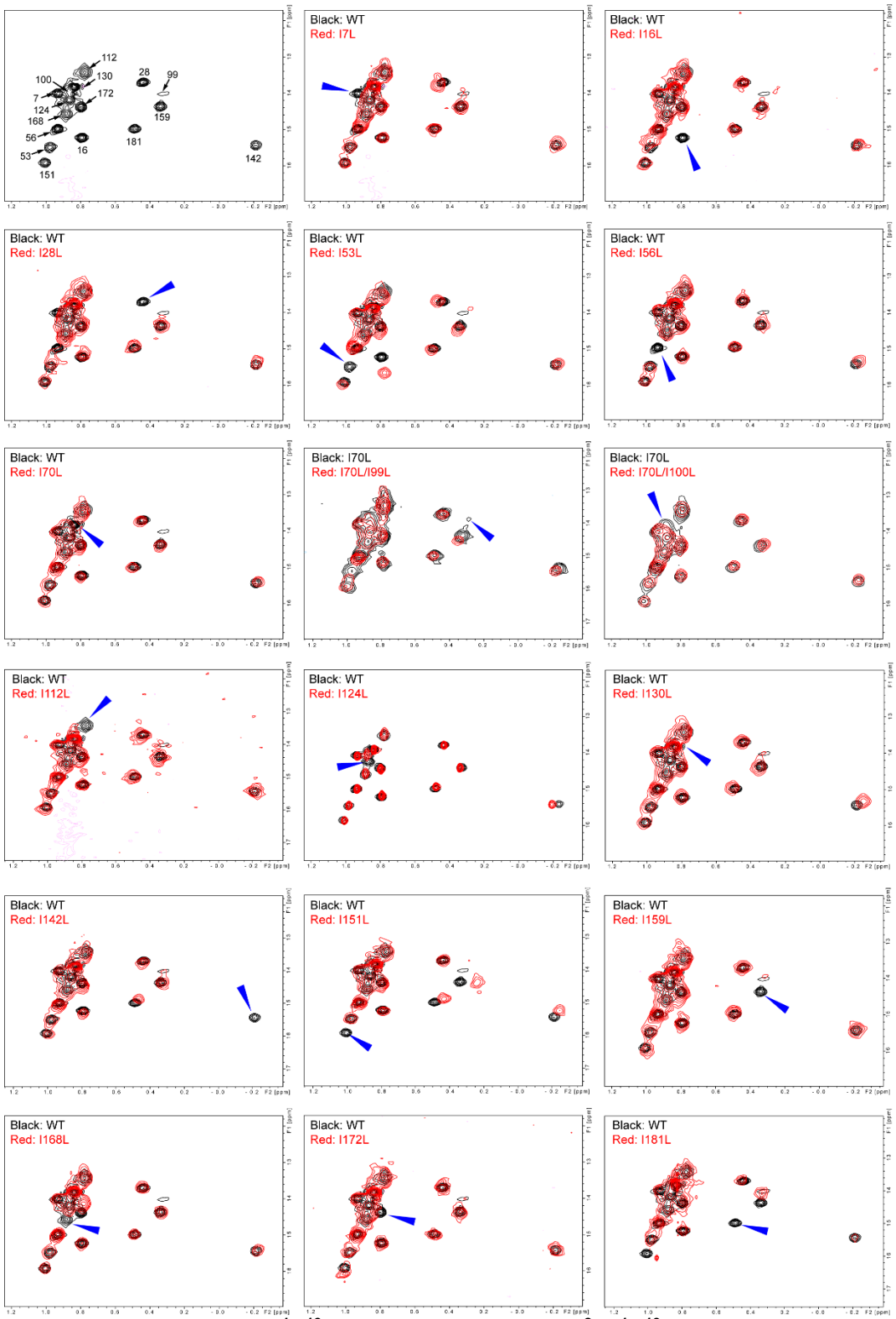

Figure S4. Assignment of the $^{1}H^{13}C$ HMQC spectrum of [U-^{2}H, $^{1}H^{13}C$-Ileδ1] QacR in the unligated state. Each mutant spectrum in red was overlaid with the corresponding reference spectrum in black. The positions of assigned resonances are indicated by blue arrow heads. For the assignment of Ile-99 and Ile-100, the double mutants, I70L/I99L and I70L/I100L were used, respectively.

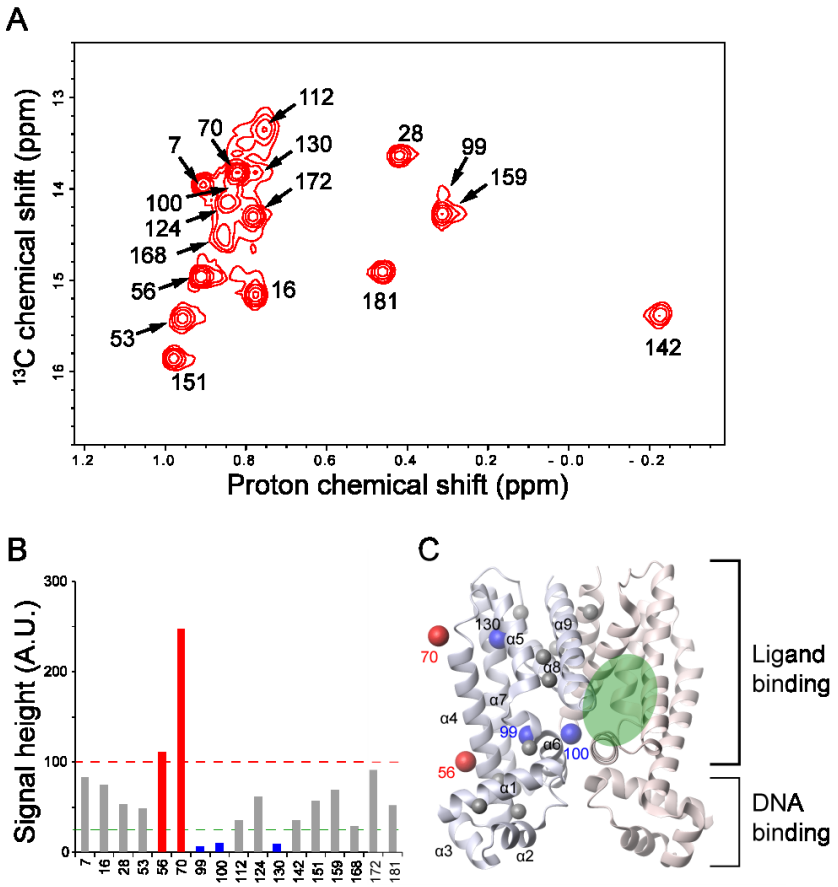

Figure S5. $^{1}H^{13}C$ HMQC spectrum of [U-^{2}H, $^{1}H^{13}C$-Ileδ1] QacR. (A) The assignments of each resonance are annotated in the $^{1}H^{13}C$ HMQC spectrum. (B) Signal height of each resonance. Note that Ile-56 and Ile70, which are exposed, show higher intensity, whereas Ile-99, Ile-100, and Ile-130, which constitute the MDB pocket, show weaker intensity. (C) The mapping of the residues with high and low intensity signals on the X-ray structure of QacR. The position of the MDB pocket is indicated in one of the dimeric subunits.

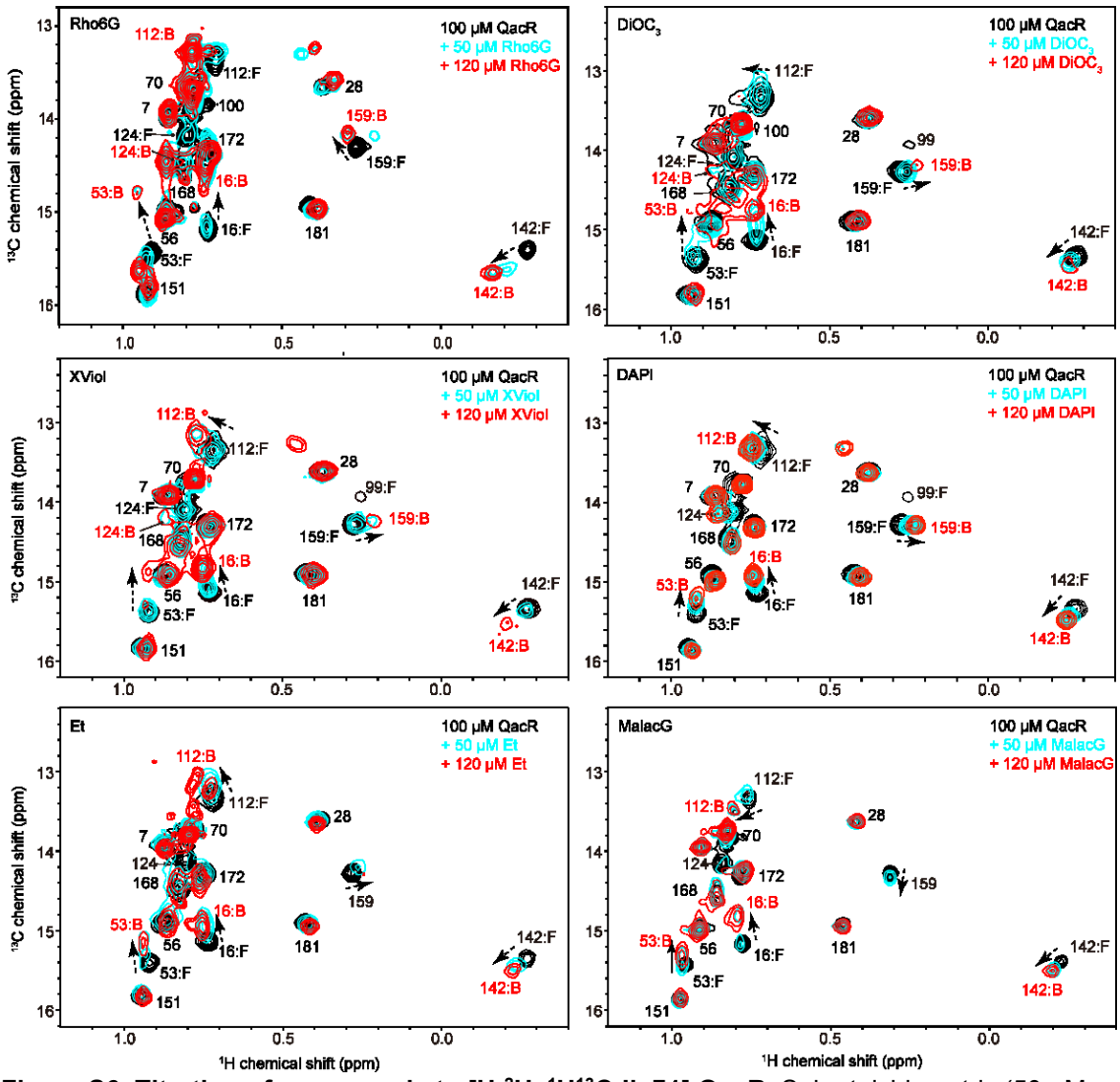

Figure S6. Titration of compounds to [U-^{2}H, ^{1}H^{13}C-Ileδ1] QacR. Sub-stoichiometric (50 μM, cyan) and excess amount (120 μM, red) of compounds were titrated to 100 μM [U-^{2}H, ^{1}H^{13}C-Ileδ1] QacR. The assignments are indicated with the corresponding states (F: unligated, B: compound bound), for those residues that showed discrete chemical shifts upon binding to the compound.

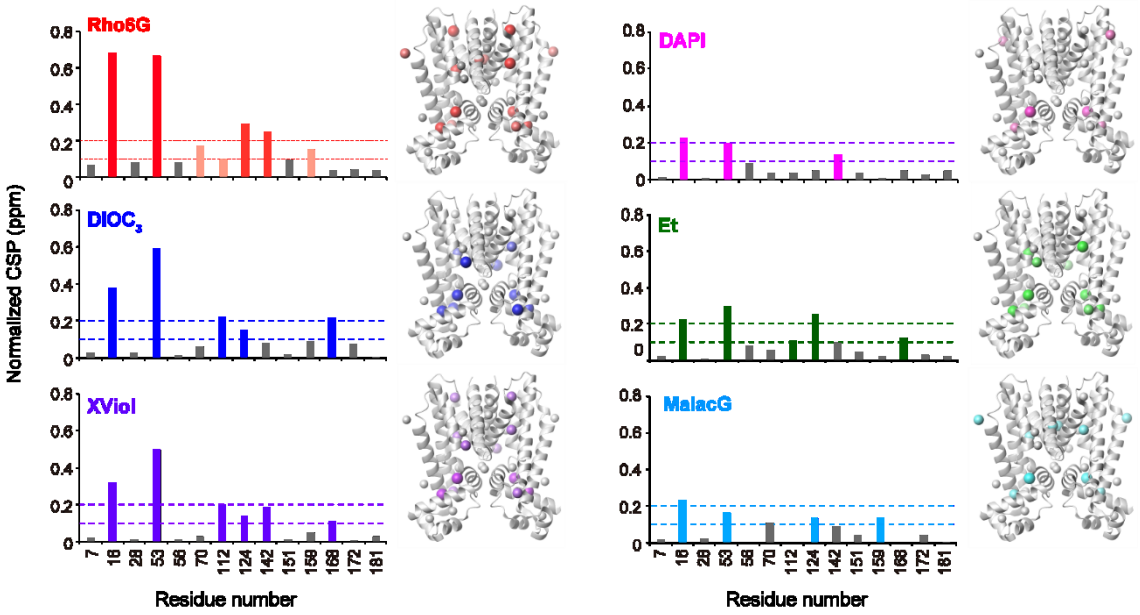

Figure S7. Comparison of chemical shift perturbations induced by compounds. Significantly perturbed (>0.1 ppm) residues are mapped on the ribbon representations of QacR in the unligated form. Rho6G and MalacG show the chemical shift change to a solvent exposed residue Ile-70. Ile-70 is located in the hinge between α4-α5 helices and in close proximity to the aromatic moiety of Trp-65, which can cause a ring current shift to Ile-70 δ1 resonance. As their relative orientations between Ile-70 and Trp-65 significantly differ between the unligated and compound bound states (Fig. R9), Ile-70 is likely sensitive to the structural change upon binding to the compounds.

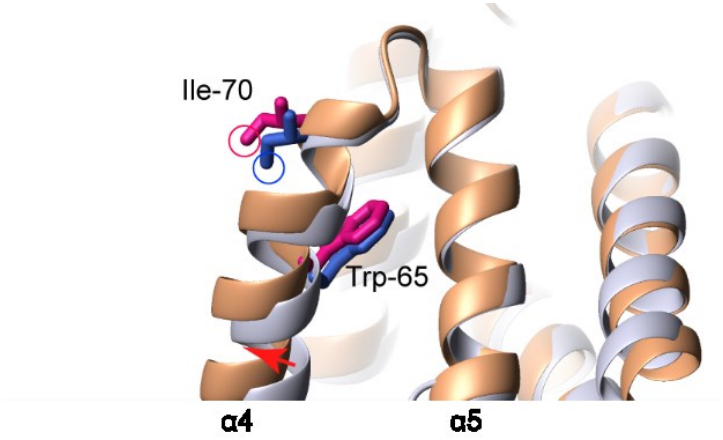

Figure S8. Positions of Ile-70 in unligated (light blue) and Rho6G-bound (brawn) states. The δ1 positions of Ile-70 in each state are circled.

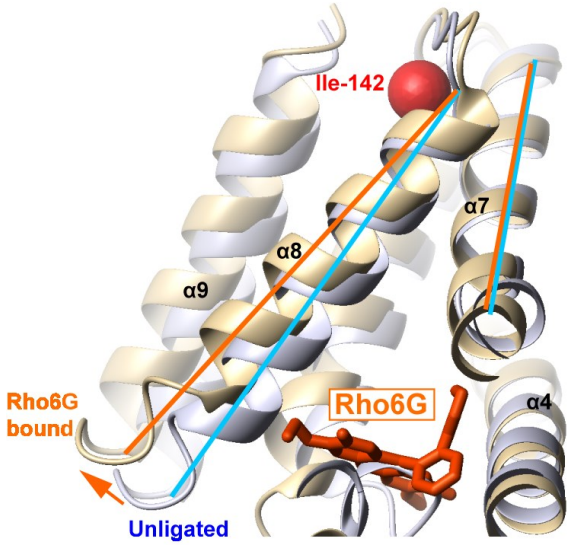

Figure S9. Enlarged view of the α7-α8 hinge, along with the positions of Ile-142 δ1. Unligated and Rho6G-bound structures are shown in blue and brown, respectively. The movement of α8 relative to α7 upon binding to the Rho6G is indicated by the arrow.

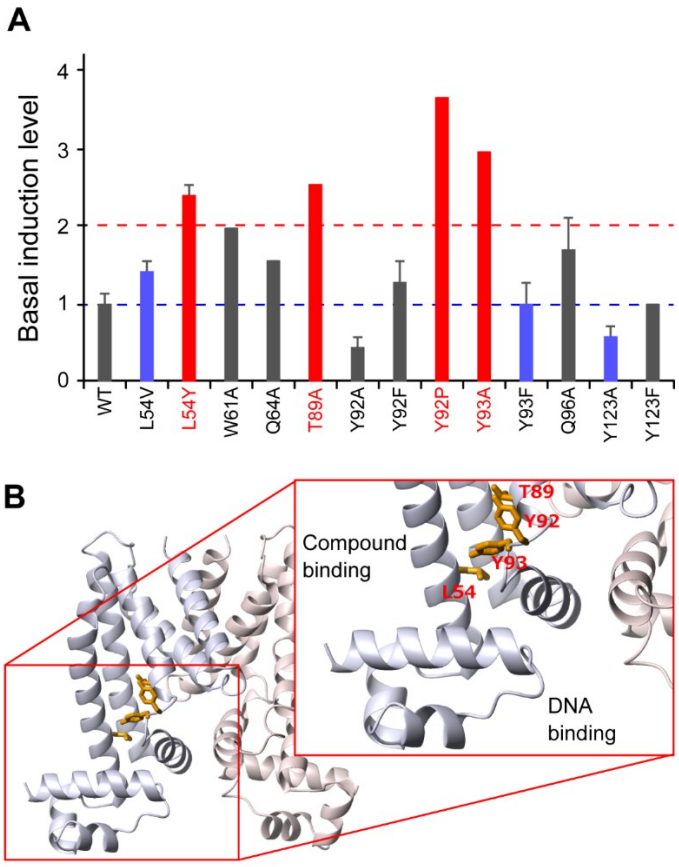

Figure S10. Constitutively active mutations of QacR. (A) Basal transcription level of QacR mutants relative to WT reported in Peters et al (3). (B) Distributions of the residues that showed >2-fold increase in the basal transcriptional activity with substitutions.

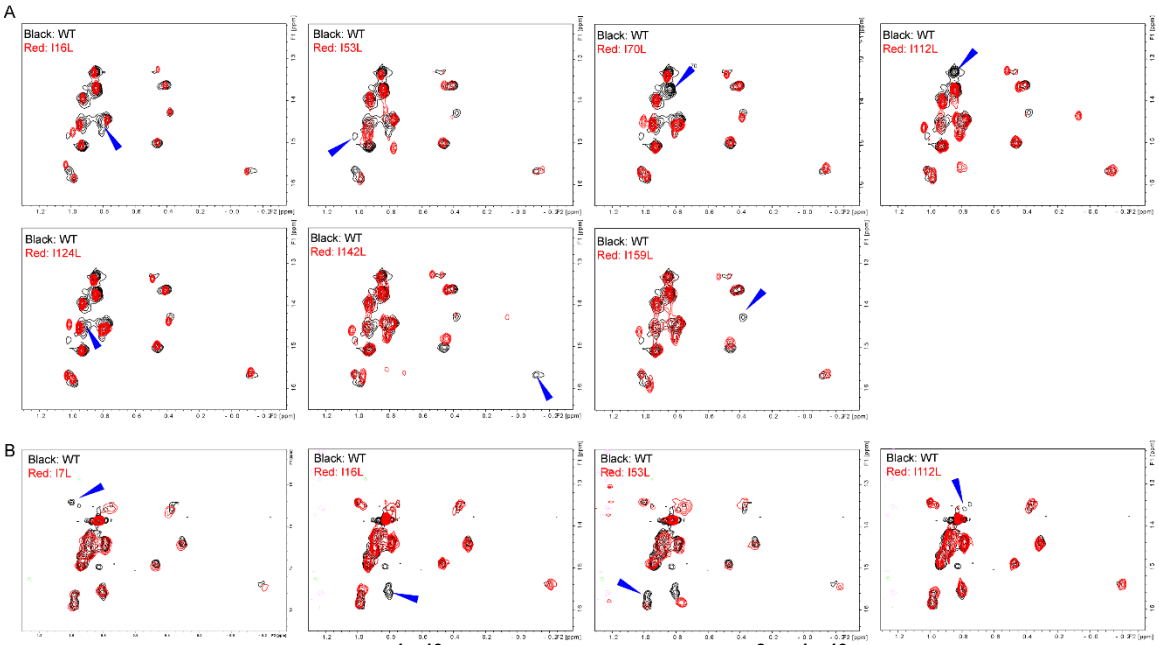

Figure S11. Assignment of the $^{1}H^{13}C$ HMQC spectrum of [U-^{2}H, $^{1}H^{13}C$-Ileδ1] QacR in (A) Rho6G-bound and (B) DNA-bound states. Each mutant spectrum in red was overlaid with the corresponding reference spectrum in black. The positions of assigned resonances are indicated by blue arrow heads.

Table S1 Chemical properties of the compound that bind and induce QacR.

Compound name	*Kd* (μM)[a]	Max induction (*x*-fold) [a]	Molecular weight[b]	Volume (Å^3)[c]
Rho6G	0.20	4.1	444	375
Crystal violet	0.30	2.4	373	350
Ethidium	0.81	1.5	314	263
DAPI	1.12	1.9	277	227
Malachite green	1.76	1.1	328	311
$DiOC_3$	1.77	3.5	362	339
Avicin	2.63	1.1	333	233
Berberine	2.88	3.1	337	246
Proflavin	3.15	1.4	209	162
Palmatine	3.74	2.7	342	281
Chelerythrine	4.08	1.1	349	270
Nitidine	4.89	2.2	349	270
Pyronin Y	5.15	1.6	268	231
Methyl green	7.04	3.2	387	382
Pheamidine	9.21	0.93	254	208
Amicarbalide	16.2	1.2	296	218
Tetraphenylarsonium	81.8	3.4	418	296

[a]The *Kd* values and maximum induction ratio were taken from Grkovic et al(2). Compounds with more than 5 consecutive methylene groups are excluded from the table. [b]Molecular weights of the compound without counter anions. [c] Volumes of the compound were calculated from their structures, using ChemSketch software (Advanced Chemistry Development).

References

1. S. Grkovic, M. H. Brown, N. J. Roberts, I. T. Paulsen, R. A. Skurray, QacR is a repressor protein that regulates expression of the Staphylococcus aureus multidrug efflux pump QacA. *J Biol Chem* **273**, 18665-18673 (1998).

2. S. Grkovic, K. M. Hardie, M. H. Brown, R. A. Skurray, Interactions of the QacR Multidrug-Binding Protein with Structurally Diverse Ligands: Implications for the Evolution of the Binding Pocket. *Biochemistry* **42**, 15226-15236 (2003).

3. K. M. Peters, G. Sharbeen, T. Theis, R. A. Skurray, M. H. Brown, Biochemical Characterization of the Multidrug Regulator QacR Distinguishes Residues That Are Crucial to Multidrug Binding and Induction of qacA Transcription. *Biochemistry* **48**, 9794-9800 (2009).